

Tracing pathways in the ocean circulation

A temperature and salinity perspective

Sara Berglund



Tracing pathways in the ocean circulation

A temperature and salinity perspective

Sara Berglund

Academic dissertation for the Degree of Doctor of Philosophy in Atmospheric Sciences and Oceanography at Stockholm University to be publicly defended on Friday 17 December 2021 at 10.00 in Magnélsalen, Kemiska övningslaboratoriet, Svante Arrhenius väg 16 B. May be moved online via Zoom, public link will then be available at the department website.

Abstract

The ocean circulation plays an essential role in our climate system. It redistributes heat, salt, carbon and other tracers across the globe, making the climate of Earth more moderate. This thesis targets density differences that are driving the ocean circulation. These differences are caused by changes in temperature and salinity. The analysis is based on the usage of Lagrangian trajectories simulated with velocity fields from an Earth System Model. The Lagrangian approach opens up for the possibility to follow specific water paths and water masses. The results herein provide a new insight to specific circulation patterns in the ocean, and which regions that play an important role in controlling temperature and salinity changes.

In the first two articles, the Lagrangian divergence is introduced. It shows the geographical distribution of heat and salt changes of a simulated water mass. Using this, we are able to show that the northward flowing water in the Atlantic Ocean cools and freshens in the North Atlantic Subtropical Gyre, the Gulf Stream and the North Atlantic Current. Similarly, we show that the water flowing from the Drake Passage, following the Antarctic Circumpolar Current (ACC) and moving northwards into the Atlantic, Pacific and Indian oceans, transforms from cold and fresh to warm and saline. This warming and salinification are a result of, not only air-sea fluxes, but also interior mixing.

In the third study, we show that 70% of the water flowing northwards as part of the Atlantic Meridional Overturning Circulation circuits the North Atlantic Subtropical Gyre at least once before it continues northwards. In the gyre, the water spirals downwards as it gets denser, due to a combination of air-sea fluxes and interior mixing. These results bring a new perspective on the Subtropical Gyre's role to the circulation patterns of the Atlantic Meridional Overturning Circulation.

In the last part of this thesis, the circulation in the North Atlantic Ocean is traced into four different pathways. The pathways are visualised geographically together with their change in temperature, salinity and density. With this, we are able to show that the northward flowing water in the Atlantic Ocean exchanges heat and salt with the colder and fresher waters circulating the Subpolar Gyre.

Keywords: *Lagrangian trajectories, Climate modelling, Atlantic Ocean, Southern Ocean, Ocean circulation, heat.*

Stockholm 2021

<http://urn.kb.se/resolve?urn=urn:nbn:se:su:diva-198210>

ISBN 978-91-7911-684-2

ISBN 978-91-7911-685-9



Stockholm
University

Department of Meteorology

Stockholm University, 106 91 Stockholm

TRACING PATHWAYS IN THE OCEAN CIRCULATION

Sara Berglund

Tracing pathways in the ocean circulation

A temperature and salinity perspective

Sara Berglund

©Sara Berglund, Stockholm University 2021

ISBN print 978-91-7911-684-2

ISBN PDF 978-91-7911-685-9

Cover image: Årstaviken, Södermalm, Stockholm city. photo: Sara Berglund, October 2021.

Printed in Sweden by Universitetsservice US-AB, Stockholm 2021

This thesis is dedicated
to my family, thank you
for always believing in
me.

"The sea, once it casts its spell,
holds one in its nets of wonder forever"
- Jacques Cousteau

Abstract

The ocean circulation plays an essential role in our climate system. It redistributes heat, salt, carbon and other tracers across the globe, making the climate of Earth more moderate. This thesis targets density differences that are driving the ocean circulation. These differences are caused by changes in temperature and salinity. The analysis is based on the usage of Lagrangian trajectories simulated with velocity fields from an Earth System Model. The Lagrangian approach opens up for the possibility to follow specific water paths and water masses. The results herein provide a new insight to specific circulation patterns in the ocean, and which regions that play an important role in controlling temperature and salinity changes.

In the first two articles, the Lagrangian divergence is introduced. It shows the geographical distribution of heat and salt changes of a simulated water mass. Using this, we are able to show that the northward flowing water in the Atlantic Ocean cools and freshens in the North Atlantic Subtropical Gyre, the Gulf Stream and the North Atlantic Current. Similarly, we show that the water flowing from the Drake Passage, following the Antarctic Circumpolar Current (ACC) and moving northwards into the Atlantic, Pacific and Indian oceans, transforms from cold and fresh to warm and saline. This warming and salinification are a result of, not only air-sea fluxes, but also interior mixing.

In the third study, we show that 70% of the water flowing northwards as part of the Atlantic Meridional Overturning Circulation (AMOC) circuits the North Atlantic Subtropical Gyre at least once before it continues northwards. In the gyre, the water spirals downwards as it gets denser, due to a combination of air-sea fluxes and interior mixing. These results bring a new perspective on the Subtropical Gyre's role to the circulation patterns of the Atlantic Meridional Overturning Circulation.

In the last part of this thesis, the circulation in the North Atlantic Ocean is traced into four different pathways. The pathways are visualised geographically together with their change in temperature, salinity and density. With this, we are able to show that the northward flowing water in the Atlantic Ocean exchanges heat and salt with the colder and fresher waters circulating the Subpolar Gyre.

Sammanfattning

Havscirkulationen spelar en betydande roll för vårt klimatsystem, bland annat genom att omfördela värme, salt, kol och andra ämnen över hela jorden och därav bidra till det klimat vi har idag. Havscirkulationen drivs av atmosfäriska vindar, samt av skillnader i densitet som uppstår då vattnets temperatur eller salinitet förändras. En förändring av vattnets temperatur och salthalt kan ske på grund av ett värme- eller färskvattenflöde genom havsytan. Det kan även ske genom att is smälter eller att vatten fryser, genom färskvatten från floder som mynnar ut i havet eller genom omblandning.

I den här avhandlingen ligger fokus på temperatur- och salthaltsförändringarna som ger upphov till densitetsskillnaderna som i sin tur driver havscirkulationen. Analysen baseras på Lagrangeska trajektorier uträknade med hjälp av hastighetsfält från en jordsystemsmodell. En jordsystemsmodell är en global klimatmodell som även beskriver biologiska och kemiska processer. En global klimatmodell beskriver klimatsystemet på jorden, exempelvis atmosfärens och havets cirkulation. Den Lagrangeska metoden innebär att man följer flera vattenpaket som rör sig med havets cirkulation. En stor fördel med metoden är att det är möjligt att spåra specifika cirkulationsmönster. Resultaten i denna avhandling tillhandahåller nya insikter om hur temperatur- och saltförändringar är kopplade till cirkulationen. Vidare bidrar resultaten till en detaljerad bild över områden i havet som har stor betydelse för drivningen av den globala havscirkulationen.

I de första två artiklarna introduceras storheten Lagrangesk divergens, som åskådliggör den geografiska fördelningen av värme- och saltförändringar för de simulerade vattenmassorna. Vi visar att det nordgående vattnet i Atlanten kyla och blir sötare, och att det till största del sker i den Nordatlantiska Subtropiska gyren, i Golfströmmen och längst den Nordatlantiska strömmen. Vatten som härrör från Drakes sund blir varmare och ökar i salinitet medan det strömmar norrut in i Atlanten, Stilla havet och Indiska oceanen. Vi visar också att förändringen av salinitet och temperatur sker genom en kombination av värme- och färskvattenflödet genom ytan samt omblandning.

I den tredje artikeln visar vi att 70% av det nordgående vattnet i Atlanten cirkulerar i den Nordatlantiska Subtropiska gyren minst ett varv innan det fortsätter norrut. I gyren rör sig vattnet nedåt likt en spiral. Det beror på att vattnet blir tyngre, vilket sker på grund av en kombination av omblandning samt ett värme- och färskvattenflöde genom ytan. Att den Subtropiska gyren spelar en så pass stor roll för den atlantiska meridionala cirkulationen (ofta kallad AMOC) kan ha stora konsekvenser i ett förändrat klimat, och det skulle därför vara av stort intresse att fortsätta undersöka dess roll.

I den sista delen av avhandlingen delar vi upp cirkulationen i Nordatlanten i fyra delar. De olika vägarna är visualiserade med hjälp av olika strömfunktioner, som visar att alla vägar på olika sätt bidrar till cirkulationen i bassängen. Vidare visar vi att det nordgående vattnet i Atlanten utbyter värme och salt med det kallare och sötare vattnet som cirkulerar i den Nordatlantiska subpolära gyren.

List of Papers

The following papers, referred to in the text by their Roman numerals, are included in this thesis.

Paper I: **Sara Berglund**, Kristofer Döös, and Jonas Nycander (2017).
Lagrangian tracing of the water–mass transformations in the Atlantic Ocean
Tellus A: Dynamic Meteorology and Oceanography, **69.1**: 1306311.
DOI: <https://doi.org/10.1080/16000870.2017.1306311>

Paper II: **Sara Berglund**, Kristofer Döös, Aitor Aldama Campino, and Jonas Nycander (2021).
The water mass transformation in the upper limb of the overturning circulation in the Southern Hemisphere
Journal of Geophysical Research: Oceans, **126.8**: e2021JC017330.
DOI: <https://doi.org/10.1029/2021JC017330>

Paper III: **Sara Berglund**, Kristofer Döös, Sjoerd Groeskamp and Trevor J. McDougall (2021).
The downward spiralling nature of the North Atlantic Subtropical Gyre
Submitted to Nature Communication, under review

Paper IV: **Sara Berglund**, Kristofer Döös, Sjoerd Groeskamp and Trevor J. McDougall (2021).
The contrasting roles of heat and salt in the overturning circulation of the North Atlantic Ocean
Manuscript

Reprints were made with permission from the publishers.

Author's contribution

For **Paper I** the idea came from the introduction of the Eulerian thermohaline stream function by Kristofer Döös. It was further developed by me, Kristofer, and Jonas Nycander during many discussions that lead to the scientific ideas and questions to ask in the paper. I made all runs with Lagrangian trajectories, collected and analysed the data and produced all the figures. I wrote the manuscript with comments from Kristofer and Jonas and did all the work for the revision before the article was accepted.

For **Paper II** the idea came as a clear continuation of Paper I. I made all different kind of Lagrangian runs with trajectories, that in the end ended up with the Drake Passage as a natural starting point. I collected and analysed the data, and made all figures. I wrote the manuscript with input from Kristofer Döös, Aitor Aldama Campino and Jonas Nycander. I did all the required revisions for publishing the paper.

The idea for **Paper III** was developed from the results of paper I. Me and Kristofer introduced the idea to Sjoerd Groeskamp and Trevor McDougall, and we together continued developing the idea. I integrated the EC-Earth3 model to generate the Eulerian fields used in the manuscript. I made the Lagrangian trajectory simulations with TRACMASS. Kristofer Döös made all figures with comments from me. I wrote the manuscript with discussion and comments from Kristofer Döös, Sjoerd Groeskamp and Trevor McDougall.

Paper IV was an idea developed during a discussion between me and Kristofer Döös on how to clearly visualise the pathways contributing to the North Atlantic Ocean circulation and its heat and salt changes. It is a broader concept of Paper I, where the entire circulation in the Atlantic Ocean is described. The data used in the study is from the EC-Earth3 simulation that I did for Paper III. The Lagrangian trajectory simulations are done by me. I produced all figures and wrote the manuscript and got input from Kristofer Döös, Trevor McDougall and Sjoerd Groeskamp.

Abbreviations

ACC	Antarctic Circumpolar Current
AMOC	Atlantic Meridional Overturning Circulation
CMIP6	Coupled Model Intercomparison Project phase 6
ECMWF	European Centre for Medium-Range Weather Forecast
ESM	Earth System Model
GCM	General Circulation Model
IFS	Integrated Forecasting System
IPCC	Intergovernmental Panel on Climate Change
MOC	Meridional Overturning Circulation
NEMO	Nucleus for European Modelling of the Ocean
OGCM	Ocean General Circulation Model

Contents

Abstract	i
Sammanfattning	ii
List of Papers	v
Author's contribution	vii
Abbreviations	ix
1 Introduction	13
2 The Ocean Circulation	15
2.1 The wind-driven circulation	15
2.1.1 Ekman, Sverdrup, Stommel and Munk	16
2.2 The thermohaline circulation	17
3 Modelling the Ocean Circulation	19
3.1 The Earth System Model EC-Earth	19
3.2 What is Lagrangian?	20
3.3 The Lagrangian trajectory model TRACMASS	21
4 Stream Functions	23
4.1 Lagrangian stream functions	24
5 The Lagrangian Divergence	27
5.1 Theory	27
5.1.1 Eulerian discretisation	28
5.1.2 Lagrangian discretisation	29
6 A summary on the Lagrangian perspective of the ocean circulation	33
6.1 The Lagrangian thermohaline stream function (Paper I and Paper II)	33
6.2 Cooling and freshening (Paper I)	33

6.3	Warming and salinification (Paper II)	34
6.4	The role of the North Atlantic Subtropical Gyre (Paper III)	36
6.5	The North Atlantic Ocean circulation (Paper IV)	36
7	Final remarks and Outlook	39
	References	xliii
	Acknowledgements	xlvi

1. Introduction

The ocean covers about 71% of the Earth's surface. It plays a crucial role in maintaining the Earth as we know it. The ocean has an essential role in controlling our climate; with its circulation and mixing it transports heat across the world making temperatures more moderate. Beyond that, the water itself is an important resource for all living organisms on Earth. It serves as a home for a large marine biodiversity, contributes to human livelihood and to human activities such as trade and transport (Bindoff *et al.*, 2019).

Tens of thousands of years ago, the starting point for understanding the ocean circulation was set when trading, travelling and new resources motivated ventures from the coast out on the sea. However, it was not until 1872 that one of the first large scientific expeditions to study the ocean took place. The *Challenger* Expedition lasted over 1000 days and collected data of currents, temperature, ocean floor deposits and water chemistry at 361 different places. The journey resulted in a scientific report of the voyage covering 29,500 pages, that took over 23 years to complete (Sverdrup *et al.*, 2005). The report is thought of as one of the ground pillars for modern oceanography.

Numerical modelling of the ocean circulation became a topic during the second half of the 20th century, and in 1969 the ocean circulation was for the first time described in a coupled atmosphere-ocean system model (Bryan, 1969, Manabe, 1969a,b). Today, we are able to study the ocean circulation and its transport of heat, salt, mass and nutrients using both numerical modelling and different types of observations, such as satellites, buoys, moorings (Cunningham *et al.*, 2007), ship measurements and even with the help of seals (Fedak, 2004).

In 1990, the first Lagrangian trajectories simulated with data from an Ocean General Circulation Model (OGCM) was developed (Van Sebille *et al.*, 2018). A Lagrangian trajectory can be thought of as the path of a water parcel in the ocean. Imagine that, instead of the traditional view where we study a field, the Lagrangian trajectories suddenly opened up a new perspective where the flow is followed instantaneously. Further, it does not only follow the flow, but can also be used to track heat, salt, and other tracers. Thus, the Lagrangian perspective makes it possible to follow the ocean circulation and simultaneously study its appurtenant transport of tracers (e.g. temperature or salinity). Today there are multiple studies every year of the ocean circulation that are based on Lagrangian trajectories (Van Sebille *et al.*, 2018).

Even though our knowledge and methods to understand the ocean have increased rapidly since the *Challenger* Expedition took place, there is still a lot to learn. The aim of this thesis is to increase the knowledge of the ocean circulation, with the main focus on temperature and salinity changes that give

rise to the density differences that drive the ocean circulation. To address this, we simulate Lagrangian trajectories using data from the ocean component of an Earth System Model (ESM). Below is a summary of the main results of the papers included in this thesis:

- In **Paper I** we show that the northward flowing water in the Atlantic Ocean loses heat and freshens in the North Atlantic Subtropical Gyre, the Gulf Stream and the North Atlantic Current.
- **Paper II** focuses on the water flowing from the Drake Passage northwards into the Atlantic, Pacific and Indian Oceans. Here we show how part of the increase in heat and salinity takes place below the mixed layer, pointing to mixing as an important factor for changes. Further, we explore the role of the mixed layer seasonality on the changes in heat and salt.
- In **Paper III** we show that 70% of the water flowing northwards as part of the Atlantic Meridional Overturning Circulation has to spiral downwards in the North Atlantic Subtropical Gyre before it is sufficiently dense to continue northwards.
- In the final paper, **Paper IV**, we put the focus on the North Atlantic Ocean, and separate the circulation into four different pathways. We show that the pathways exchange heat and salt with each other, and that they all are necessary for the heat and salt variations in the North Atlantic Ocean.

2. The Ocean Circulation

The ocean circulation is often separated into two constituents that are driven by different forcing mechanisms; the wind-driven circulation and the thermohaline circulation. However, these are intertwined and thus jointly drive the circulation. Therefore, a change in the wind-driven system will alter the thermohaline circulation, and a change in the thermohaline forcing will alter the wind-driven currents. Figure 2.1 shows a schematic of the global ocean circulation, including both the formation of deep waters and the wind-driven gyres.

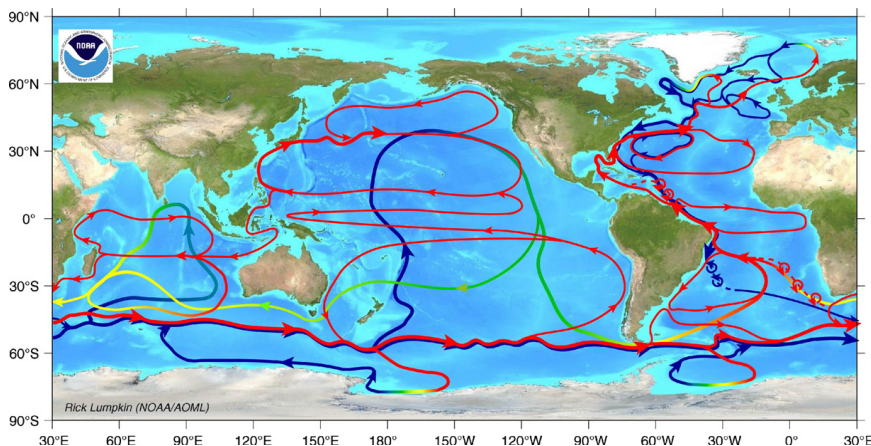


Figure 2.1: The ocean circulation. Colours indicate depth of the circulation; red – surface, green/yellow – intermediate, blue – deep. Figure from Richardson (2008).

2.1 The wind-driven circulation

Surface currents are created as atmospheric winds "drag" the ocean surface. Once the surface of the ocean is set into motion, a relatively constant surface current circulation is created (Figure 2.2). This circulation pattern includes the gyre circulations, which also encompass the western boundary currents. One example of a western boundary current is the Gulf Stream. Figure 2.2 shows five Subtropical Gyres and two Subpolar Gyres; one in the North Atlantic

Ocean and one in the North Pacific Ocean. In the Southern Ocean, where no continents block the ocean, the Antarctic Circumpolar Current (ACC) transports water around Antarctica (Figure 2.2). The Weddell and Ross Gyres are also Subpolar Gyres, but not marked explicitly in Figure 2.2, but can be seen as two re-circulations in the Southern Ocean.

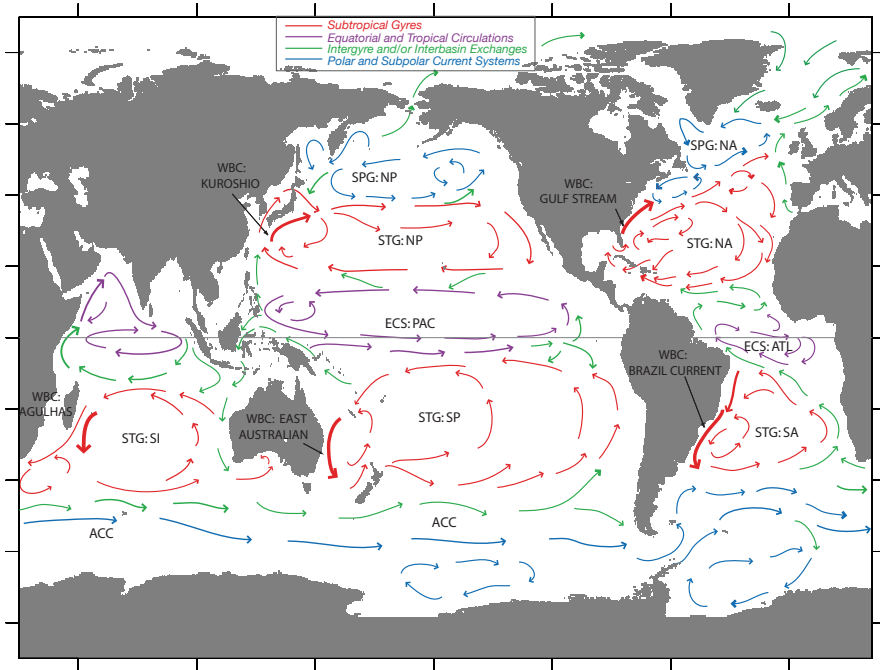


Figure 2.2: The wind-driven circulation of the ocean, from Vallis (2017). It shows five Subtropical Gyres (STG; red arrows) with their western boundary currents, three equatorial circulations (ECS; purple arrows), with their undercurrents, and three polar and subpolar currents (Subpolar Gyres - SPG and the Antarctic Circumpolar Current - ACC; blue arrows). Finally, green arrows show the inter-gyre circulation.

2.1.1 Ekman, Sverdrup, Stommel and Munk

The effect of the winds (called the wind stress) reaches only a few tens of metres below the surface; namely through the *Ekman layer*. In the conceptual model of Ekman (1905) the layer just below the surface is set into motion, but is deflected to the right (in the Northern Hemisphere). This deflection results in the *Ekman spiral*. The average flow of water over the spiral will move 90° to the right (in the Northern Hemisphere) of the wind stress. At the base of the Ekman layer, Ekman (1905) described the vertical upwelling velocity as:

$$w_{Ek} = \mathbf{k} \cdot \nabla \times \frac{\tau_S}{\rho_0 f}, \quad (2.1)$$

where f is the Coriolis parameter, ρ_0 is the density of sea water, \mathbf{k} is the unit vertical vector and τ_S is the surface wind stress vector.

In 1947, Sverdrup (1947) showed that the depth-integrated meridional velocity was proportional to the wind stress curl, and created a conceptual model of the gyre circulation, the *Sverdrup Balance* was thus derived as:

$$\beta \int v dz = \frac{1}{\rho_0} \mathbf{k} \cdot \nabla \times \tau_S, \quad (2.2)$$

where β is the variation with latitude of the vertical component of the planetary vorticity and v is the meridional velocity.

Stommel (1948) further developed the gyre circulation solution by adding a linear drag. This prohibited the input of vorticity by the surface wind stress curl and allowed for the return flow of the western boundary current. This was extended by Munk (1950), who added a no-slip boundary condition and a lateral friction to the solution.

These theories set the base of the wind-driven ocean circulation, and are still a ground pillar to our understanding of the circulation within gyres. There has been tremendous work on the gyre circulations that has increased our knowledge from these first studies, but as climate models evolve, and the observational data coverage increases we continue to learn.

2.2 The thermohaline circulation

The ocean circulation that is driven by differences in density is known as the thermohaline circulation. As the name entails, the changes in density are controlled by the changes in temperature and salinity. The density differences caused by a change in temperature and/or salinity create an overturning circulation. Waters that are cooled and/or salinified at the surface become dense and sink (Sandström, 1908). Due to conservation of mass, this sinking water will be replaced by new water transported in at the surface. Finally, deep water upwells in other regions as a result of turbulence and winds, closing the overturning circulation. The thermohaline circulation is thus forced by turbulent mixing and thermohaline forcing at the surface (Rahmstorf, 2003).

The sea surface temperature and salinity can be changed by heat or freshwater exchange with the atmosphere (e.g. evaporation or precipitation). The formation and melt of sea ice, as well as river runoff, also change the temperature and salinity distribution of waters, mainly through the exchange of freshwater. The structure of the surface salinity and temperature is further driven by vigorous surface mixing and advection. Below the surface layer, at depths where the water no longer is affected by the atmosphere, interior mixing causes changes in temperature and salinity.

The thermohaline circulation is sometimes confused with the Meridional Overturning Circulation (MOC) of the ocean. However, the MOC is the zonal

integral of the meridional and vertical circulation (Vallis, 2017). This means that both the thermohaline circulation and the wind-driven circulation contributes to the total MOC. The MOC can be reduced to the Atlantic Meridional Overturning Circulation (AMOC), which describes the overturning circulation in the Atlantic Ocean. The AMOC is depicted in Figure 2.1 as follows; surface water is transported into the Atlantic Ocean from the Agulhas current system and the Drake Passage. As the water crosses the equator and enters the North Atlantic Ocean it cools and freshens. In the northernmost parts, the water is dense and thus sinks. At depths it returns south towards the Southern Ocean, where it upwells as a result of winds and turbulence (Lozier, 2012).

The AMOC transports large amounts of heat from low to high latitudes, contributing to the relatively mild climate in Europe. It also acts as a reservoir for atmospheric CO₂, due to its uptake and ventilation of anthropogenic greenhouse gases (Lozier, 2012). Several studies have shown that the AMOC has slowed down during the 20th century (Caesar *et al.*, 2021, Rahmstorf *et al.*, 2015), and is predicted to further do so, but to what extent, and what consequences this may bring is yet not known (Bindoff *et al.*, 2019, Weijer *et al.*, 2020). In **Paper I** and **Paper III** the upper water flowing northwards as part of the AMOC is studied, while in **Paper IV** waters in the North Atlantic Ocean that are part of the AMOC are studied.

3. Modelling the Ocean Circulation

General Circulation Models (GCM) or Earth System Models (ESM) are of great importance for scientists to be able to predict and understand the Earth's climate. The difference between a GCM and an ESM is sometimes unclear, but the general idea is that an ESM includes components covering biophysical and biogeochemical processes, and often a more complex aerosol treatment. An Ocean General Circulation Model (OGCM), is used to represent the ocean and its behaviour. An OGCM consists of small boxes (grid boxes), in which dynamical and physical processes of the ocean are represented. Processes that are too small to scale into a grid box are usually parameterised, for example eddies, internal waves, double-diffusion, turbulence. There are non-eddy, eddy-permitting and eddy-resolving ocean models, depending on the horizontal resolution, where the latter has such a fine resolution that the small-scale eddies are resolved. The horizontal and vertical resolution of an OGCM are set by the size of the grid boxes.

Over the past decades, climate modelling has evolved as the understanding of the climate system has increased. The representation of processes improves continuously as high-resolution models are developed and as parameterisation schemes are improved. In the latest report from the Intergovernmental Panel of Climate Change (IPCC) the ESMs applied to predict climate change mainly include ocean models that are non-eddy (Chen *et al.*, 2021). However, there is also a large community working on improving the resolution of ESMs, including eddy-resolving ocean models (Fedak, 2004, Haarsma *et al.*, 2016).

In **Paper I** and **Paper II** data from the ocean component Nucleus for European Modelling of the Ocean (NEMO) of the ESM EC-Earth2 were used. The resolution applied for NEMO is 1° with 42 depth levels and monthly mean outputs, thus it is a non-eddy model. For **Paper III** and **Paper IV** the ESM EC-Earth3 was integrated following the guidelines of the Coupled Model Intercomparison Project Phase 6 (CMIP6), and data from the ocean model NEMO3.6 were used. This version of NEMO is still non-eddy, but has an increased vertical resolution with 75 depth levels.

3.1 The Earth System Model EC-Earth

The following applies to EC-Earth3, but there are many similarities to EC-Earth2. EC-Earth3 exists in different coupled configurations, and in this thesis

the EC-Earth-Veg version 3.3.1.1 is integrated. EC-Earth3 follows the concept "seamless prediction", which means that the atmospheric model used is adapted from the European Centre for Medium-Range Weather Forecasts (ECMWF) seasonal prediction system S4 (Döscher *et al.*, 2021). The idea with this is to be able to simulate climate predictions similarly as seasonal predictions, since the difference between them mainly are the difference in time scales (Brunet *et al.*, 2010). The atmospheric model of EC-Earth3 is the Integrated Forecasting System cycle 36r4 (IFS 36r4) from ECMWF. Further, EC-Earth3 uses the surface module HTESSEL, the ocean model NEMO3.6 and the sea-ice module LIM3. Variables are coupled with the OASIS3-MCT coupler. In EC-Earth-Veg the extra interactive vegetation model LPJ-GUESS is active. The resolution of the atmospheric model IFS 36r4 is T255L91 (≈ 80 km), while the ocean resolution is ORCA1L75 (1° and 75 depth levels). The ORCA grid is tri-polar, which means that it consists of three poles, resulting in a slightly varying horizontal resolution. The time step used for each computation within a grid box is 2700 seconds (Döscher *et al.*, 2021).

3.2 What is Lagrangian?

Imagine yourself at a football stadium, and your team gets a penalty. You are sitting in the audience, watching how the penalty is taken by your favourite player and you see how the ball ends up in the goal. You are thus watching everything that happens from a fixed point in space (i.e. *Eulerian*¹). Now, instead imagine you are the ball (maybe hard to imagine, but let's try!). As the player kicks you (well, the ball) you fly away over the pitch and into the goal, you are thus seeing everything from the perspective of the ball (i.e. *Lagrangian*²). The path of the ball from the penalty point to the goal constitutes a *Lagrangian trajectory*.

Now, let us translate this into the flow of waters. In the Eulerian framework we could for example anchor a buoy in a specific location and observe how temperature changes in time at its location. In the Lagrangian framework, we would instead release a free-floating buoy and measure the temperature as the buoy moves with the flow. The pathway of the buoy would then be the *Lagrangian trajectory*.

We can hence describe a flow from two different viewpoints. But, why is this of any interest? An advantage with the Lagrangian view is that it is possible to follow parcels of particular interest, instead of looking at snapshots of fields. It further makes it possible to select specific water masses or circulations to study in detail, which is not as straight forward with the Eulerian view. The results in this thesis are entirely originating from a Lagrangian viewpoint, where Lagrangian trajectories are computed and used to understand different ocean circulation patterns and their attributed heat and salt changes.

¹From Leonhard Euler

²From Joseph Louis Lagrange

3.3 The Lagrangian trajectory model TRACMASS

The Lagrangian trajectory model TRACMASS is used to calculate Lagrangian trajectories. The TRACMASS scheme was originally introduced for stationary velocity fields by Döös (1995) and Blanke & Raynaud (1997). Further on, de Vries & Döös (2001) extended the scheme for time-dependent fields. The main purpose with TRACMASS is to compute the path of a parcel. To do so, the velocity field has to be known. As of today, TRACMASS can be used both for the atmosphere and the ocean, either with different ESMs or satellite data such as AVISO (TRACMASS, 2021). Most ESMs use some sort of curvilinear or spherical grids, which means that their spherical coordinates will be functions of locations, and thus vary zonally and meridionally. TRACMASS uses volume transports, instead of velocities, to compute trajectory paths, and therefore both curvilinear and spherical grids are represented in the scheme. At the eastern and northern wall of a grid-box (i, j, k) at time step t , the volume transport is given by:

$$U_{i,j,k,t} = u_{i,j,k,t} \Delta y_{i,j} \Delta z_{i,j,k,t}, \quad (3.1)$$

$$V_{i,j,k,t} = v_{i,j,k,t} \Delta x_{i,j} \Delta z_{i,j,k,t}, \quad (3.2)$$

where $u_{i,j,k,t}$ and $v_{i,j,k,t}$ are the zonal and meridional velocities through the grid box (i, j, k) , $\Delta x_{i,j}$ and $\Delta y_{i,j}$ are the longitudinal and latitudinal grid lengths, and $\Delta z_{i,j,k,t}$ is the vertical level thickness. The vertical volume transport through the upper face of grid box (i, j, k) can be computed by the vertical velocity $w_{i,j,k,t}$. However, as TRACMASS relies on volume continuity, and in order to be certain to respect this volume conservation, it is more suitable to compute the vertical volume transport from the continuity equation. The vertical volume transport through the upper face of the grid box is:

$$W_{i,j,k-1,t} = W_{i,j,k,t} - [U_{i,j,k,t} - U_{i-1,j,k,t} + V_{i,j,k,t} - V_{i,j-1,k,t} + \frac{\Delta z_{i,j,k,t} - \Delta z_{i,j,k,t-1}}{\Delta t_G} \Delta x_{i,j} \Delta y_{i,j}], \quad (3.3)$$

where incompressibility is assumed. Δt_G is the time between two ESM fields.

There are two options of computing Lagrangian trajectories in TRACMASS, either by a step-wise scheme or by a time-dependent scheme. The first is mainly made for stationary fields, but can however be used for time-dependent fields by assuming that the field is stationary between two time steps. The latter instead takes into account the time-dependency of the fields, where a differential equation is solved based on linear interpolation in both space and time. Döös *et al.* (2017a) evaluated the schemes and showed a better accuracy when using the time-dependent scheme compared to the step-wise. However, if choosing long enough intermediate time steps, the step-wise solution will converge towards the time-dependent.

TRACMASS is volume/mass conserving. This results from the fact that transports only are linearly integrated between the grid box walls, and that

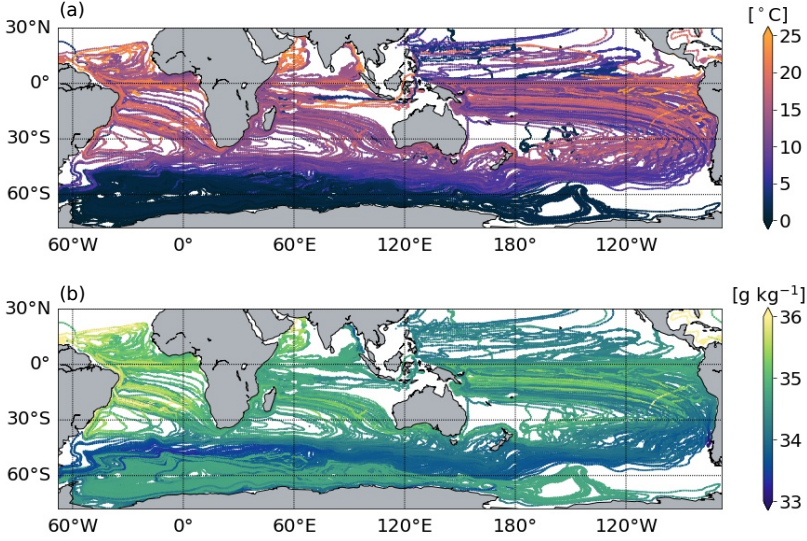


Figure 3.1: Lagrangian trajectories computed with the TRACMASS scheme. The trajectories start in the Drake Passage and end in the Atlantic, Pacific or Indian oceans as they reach the 25°C isotherm. (a) A portion of the trajectories reaching the 25°C isotherm, coloured according to their temperature. (b) Same but coloured after salinity. Figure adapted from **Paper II**.

the transports are handled in the same manner as in an ESM. The latter refers to that the TRACMASS scheme computes the vertical transport directly from the continuity equation, which is the same approach applied in most ESMs. That the scheme is mass conserving means that the sum of all trajectory fluxes in and out of a grid box is exactly zero. This also prevents trajectories in TRACMASS to cross any solid boundaries, such as a coast or the bottom of the ocean.

As trajectories are integrated, temperature, salinity and density from the ESM can be saved continuously. Similarly, any other tracer from an ESM can be saved together with the trajectories. Tracers in TRACMASS are interpolated in time between two Eulerian fields. If a tracer is saved on a grid wall it can further be interpolated in space between the two nearest grid boxes.

Figure 3.1 shows a portion of the trajectories simulated in **Paper II** from the Drake Passage until they reach the 25°C isotherm. They are coloured according to their temperature and salinity.

4. Stream Functions

Stream functions have been proved to be a valuable tool for scientists, mainly as they can explain the complexity of a circulation system in a two dimensional figure. The stream functions in this thesis are computed to describe volume transports and are given in Sverdrup ($1 \text{ Sv} \equiv 10^6 \text{ m}^3 \text{ s}^{-1}$). A frequently used stream function in oceanography is the meridional overturning stream function (Vallis, 2017), which shows the zonally integrated circulation across latitudes. It is often used as a measure for the AMOC (Buckley & Marshall, 2016), where the maximum value sets the strength of the circulation.

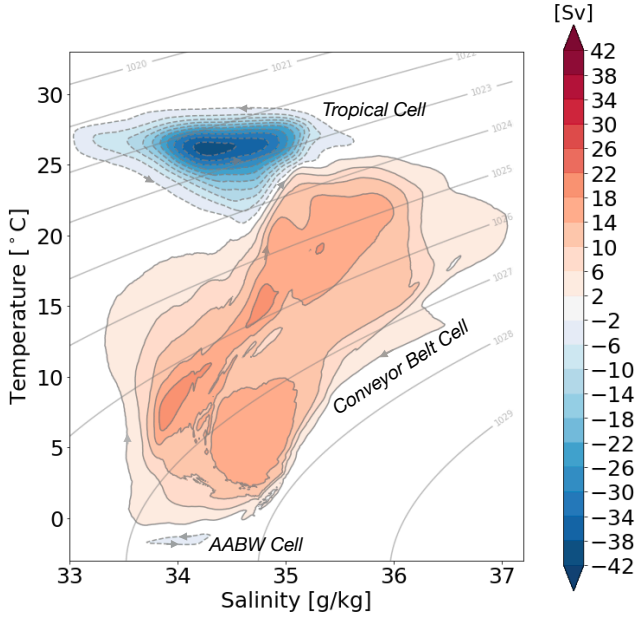


Figure 4.1: The thermohaline stream function adapted from **Paper I**. The stream function constitutes three cells: The Tropical Cell, The Conveyor Belt Cell and The Antarctic Bottom Water (AABW) Cell. The Conveyor Belt Cell has a clockwise circulation, while the Tropical Cell and the AABW Cell are anti-clockwise.

Different combinations of stream functions can give details of the flow in different perspectives. An example of this is shown by Döös & Webb (1994) who studied the Deacon Cell using stream functions in a latitude-depth, latitude-

density and depth-density space. They showed that the Deacon Cell is mainly an overturning cell in depth along density surfaces, thus in latitude-density space it does not show up.

In 2012, Döös *et al.* (2012) and Zika *et al.* (2012) introduced the thermohaline stream function in two separate studies. The stream function consists of two tracer coordinates, namely temperature and salinity. Groeskamp *et al.* (2014) further extended the stream function for moving isohalines and isotherms. Since the ocean circulation is partly driven by differences in density, arising from temperature and salinity changes, it is advantageous to study the circulation from this perspective. The draw-back, on the other hand, is that any connection to the geographical space is lost.

Döös *et al.* (2012) showed that the stream function consists of three cells; (1) The Conveyor Belt Cell, (2) The Tropical Cell and (3) The Antarctic Bottom Water (AABW)¹ Cell (Figure 4.1). **Paper I** and **Paper II** focus on the Conveyor Belt Cell, which describes a clockwise circulation in temperature-salinity space. It consists of one cooling and one warming branch. The former is suggested by Döös *et al.* (2012) to describe the upper branch of the AMOC, where air-sea interaction cools and freshens the water. Döös *et al.* (2012) further suggested the warming branch to include water moving with the Ekman transport northwards in the Southern Ocean, warming and salinifying due to heat and freshwater fluxes through the sea surface.

There are several studies that successfully have applied stream functions in different coordinate systems to explain the ocean circulation (*e.g.* Aldama Campino (2019), Aldama Campino *et al.* (2020), Döös & Webb (1994), Döös *et al.* (2012, 2017b), Groeskamp *et al.* (2014), Hieronymus *et al.* (2014), Nycander *et al.* (2007), Zika *et al.* (2012)).

4.1 Lagrangian stream functions

As the TRACMASS scheme is mass (or volume) conserving, it is possible to compute Lagrangian stream functions from selected trajectories. This can be done for any stream function, both geographically and with tracers, by using the parcels volume transport. The concept of Lagrangian stream functions were firstly introduced by Blanke *et al.* (1999), and has thereafter been applied in many studies following (*e.g.* Döös *et al.* (2008), Drijfhout *et al.* (2003), Friocourt *et al.* (2005), Thomas *et al.* (2015)).

Figure 4.2 schematically describes one trajectory n , with the volume transport F_n , passing through a grid box. All trajectories entering a grid box will also leave it and each individual trajectory's volume transport is conserved. Due to that, the total transport field will exactly satisfy:

$$F_{i,j,k}^x - F_{i-1,j,k}^x + F_{i,j,k}^y - F_{i,j-1,k}^y + F_{i,j,k-1}^z - F_{i,j,k}^z = 0, \quad (4.1)$$

where F^x , F^y and F^z are the zonal, meridional and vertical volume flux respectively. This field can be integrated either vertically, meridionally or zonally to

¹The Antarctic Bottom Water is a water mass formed in the Southern Ocean.

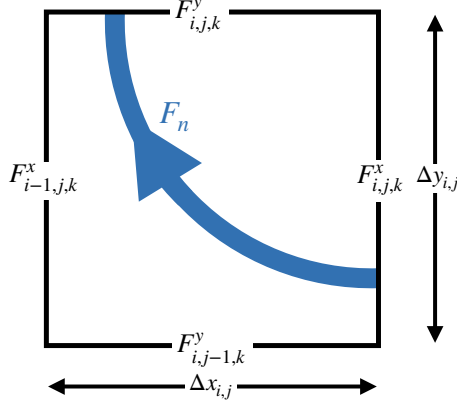


Figure 4.2: One trajectory denoted n passing through a grid box with its volume transport F_n . The figure is adapted from Döös *et al.* (2017a).

obtain a set of Lagrangian stream functions describing the flow of the selected waters.

The Lagrangian barotropic stream function can be computed as follows:

$$\psi_{i,j} = \psi_{i-1,j} + \sum_k \sum_n F_{i,j,k,n}^y, \quad (4.2)$$

$$\psi_{i,j} = \psi_{i,j-1} - \sum_k \sum_n F_{i,j,k,n}^x, \quad (4.3)$$

where $F_{i,j,k,n}^y$ is the meridional volume transport of trajectory n and $F_{i,j,k,n}^x$ is the zonal volume transport of trajectory n . i, j and k are the zonal, meridional and vertical indices of the trajectory.

The Lagrangian meridional overturning stream function is computed as follows:

$$\psi_{j,k} = \psi_{j-1,k} + \sum_i \sum_n F_{i,j,k,n}^z, \quad (4.4)$$

$$\psi_{j,k} = \psi_{j,k-1} - \sum_i \sum_n F_{i,j,k,n}^y, \quad (4.5)$$

where $F_{i,j,k,n}^y$ and $F_{i,j,k,n}^z$ are the meridional and vertical volume transport of trajectory n .

If temperature and salinity are saved along the Lagrangian trajectories, it is also possible to compute tracer-latitude stream functions as follows:

$$\psi_{j,m} = \psi_{j-1,m} - \sum_i \sum_n F_{i,j,m,n}^m, \quad (4.6)$$

$$\psi_{j,m} = \psi_{j,m-1} - \sum_i \sum_n F_{i,j,m,n}^y, \quad (4.7)$$

where $F_{i,j,m,n}^y$ is the meridional volume flux, while $F_{i,j,m,n}^m$ is the volume flux across isolines of the tracer. m is the index of the isoline.

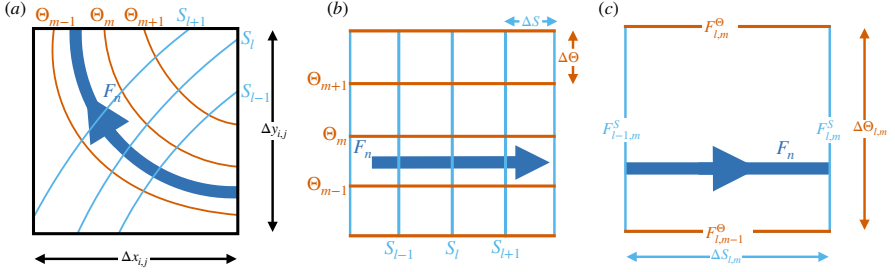


Figure 4.3: One trajectory denoted n passing through a grid box with its volume transport F_n . Θ denote isotherms which are coloured red, while S denote isohalines and are coloured blue. (b) shows the same trajectory but only projected in temperature-salinity space. (c) A zoom-in on one temperature-salinity grid box that the trajectory passes through. The flux through the isotherms are here defined to be zero $F_{l,m}^\Theta = F_{l,m-1}^\Theta = 0$, while the flux through the isohalines are $F_{l,m}^S = F_{l-1,m}^S = F_n$.

Finally, trajectories can be used to compute the Lagrangian thermohaline stream function. This is schematically described in Figure 4.3. The computation is performed by integrating trajectories in temperature-salinity space (Figure 4.3), as follows:

$$\psi_{l,m} = \psi_{l,m-1} + \sum_n F_{l,m,n}^S, \quad (4.8)$$

$$\psi_{l,m} = \psi_{l-1,m} - \sum_n F_{l,m,n}^\Theta, \quad (4.9)$$

where $F_{l,m,n}^S$ and $F_{l,m,n}^\Theta$ are the volume transports at constant isohalines and isotherms.

5. The Lagrangian Divergence

The Lagrangian divergence of heat and salt was introduced in **Paper I**, and further developed in **Paper II** for mixed layer depths, and applied to density (σ_0) in **Paper III**. It ultimately describes changes in heat, salt or density that results from horizontal diffusion, vertical diffusion or surface forcing (*e.g.* evaporation, precipitation, heat flux).

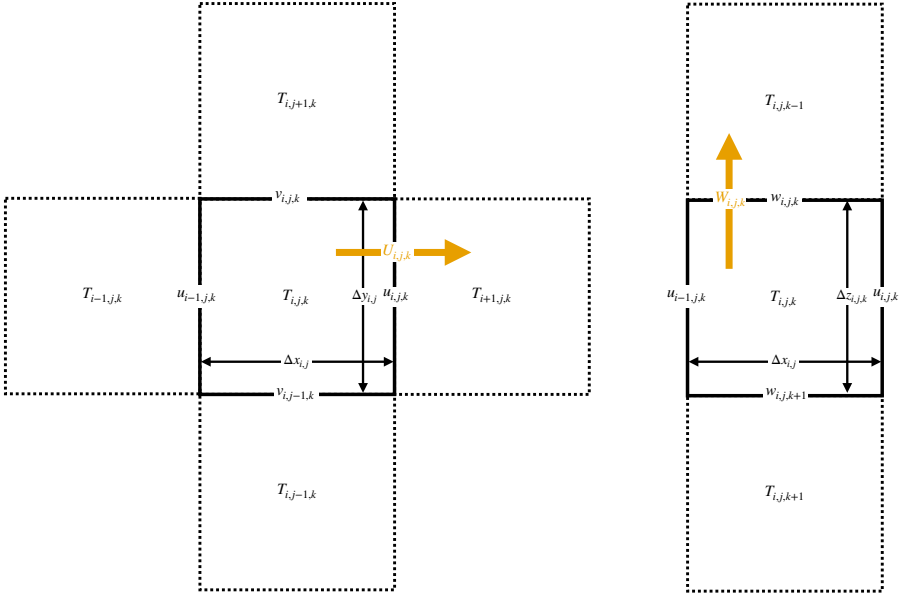


Figure 5.1: Description of the discretisation of the tracer equation. $U_{i,j,k}$, $V_{i,j,k}$ and $W_{i,j,k}$ are the zonal, meridional and vertical tracer fluxes across grid walls. Adapted from Döös *et al.* (2021)

5.1 Theory

The Lagrangian divergence was developed from the Eulerian perspective of the evolution of a tracer. The tracer conservation equation can be written as follows:

$$\frac{\partial T}{\partial t} + \mathbf{V} \cdot \nabla T = D^T + F^T, \quad (5.1)$$

where T is the tracer, D^T is the horizontal and vertical diffusion, and \mathbf{V} is the three-dimensional velocity component (u, v, w) . The local rate of change of the tracer is set by $\partial T / \partial t$. F^T is a surface forcing term, *e.g.* heat or fresh-water fluxes through the sea surface, river runoff, the exchange of heat, salt and freshwater with sea ice, or exchange through the sea floor. The most pronounced source is the flux through the sea surface, whilst river runoff and the ocean-sea-ice exchange can be regionally large.

If using an ocean model that is incompressible (*e.g.* NEMO), the following is applicable for the continuity equation:

$$\nabla \cdot \mathbf{V} = \frac{\partial u}{\partial x} + \frac{\partial v}{\partial y} + \frac{\partial w}{\partial z} = 0. \quad (5.2)$$

Equation (5.1) can, with the use of Equation (5.2), be re-written as follows:

$$\frac{\partial T}{\partial t} + \nabla \cdot (\mathbf{V}T) = D^T + F^T. \quad (5.3)$$

The term $\nabla \cdot (\mathbf{V}T)$ now describes the the divergence of the tracer flux. By assuming that the average rate of change of the tracer is much smaller than the average divergence term over a long simulation (*e.g.* an historical simulation), Equation (5.3) can be simplified to:

$$\nabla \cdot (\mathbf{V}T) \approx D^T + F^T. \quad (5.4)$$

This means that the divergence of a tracer is approximately the sum of the diffusion and surface forcing terms.

5.1.1 Eulerian discretisation

The discretisation of the divergence term is applied by looking at the sum of all tracer transports in and out of a grid box and divide them by the volume of the grid box (Figure 5.1). The tracer flux across a grid wall is computed as follows:

$$U_{i,j,k,t} = u_{i,j,k,t} \frac{1}{2} (T_{i,j,k,t} + T_{i+1,j,k,t}) \Delta y_{i,j} \Delta z_{i,j,k,t}, \quad (5.5)$$

$$V_{i,j,k,t} = v_{i,j,k,t} \frac{1}{2} (T_{i,j,k,t} + T_{i,j+1,k,t}) \Delta x_{i,j} \Delta z_{i,j,k,t}, \quad (5.6)$$

$$W_{i,j,k,t} = w_{i,j,k,t} \frac{1}{2} (T_{i,j,k,t} + T_{i,j,k-1,t}) \Delta x_{i,j} \Delta y_{i,j}, \quad (5.7)$$

where $u_{i,j,k,t}$, $v_{i,j,k,t}$ and $w_{i,j,k,t}$ are the zonal, meridional and vertical velocities and t is the time-index. The divergence of tracer T is then discretised accordingly:

$$\nabla \cdot (\mathbf{VT})_{i,j,k,t} \approx \frac{(U_{i,j,k,t} - U_{i-1,j,k,t} + V_{i,j,k,t} - V_{i,j-1,k,t} + W_{i,j,k-1,t} - W_{i,j,k,t})}{\Delta x_{i,j} \Delta y_{i,j} \Delta z_{i,j,k,t}}. \quad (5.8)$$

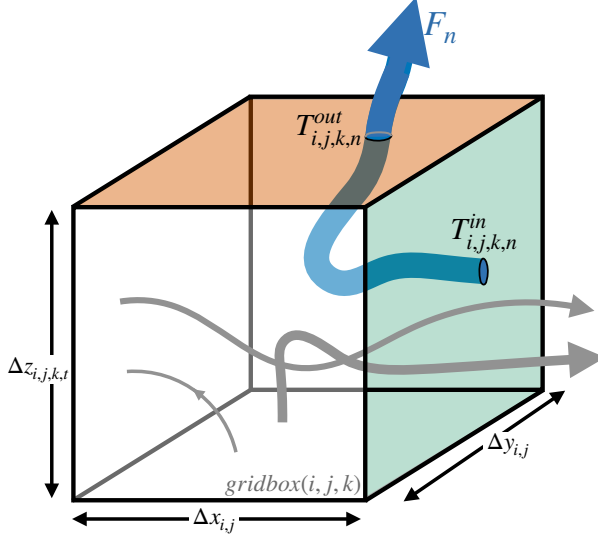


Figure 5.2: A grid-box (i, j, k) with a Lagrangian trajectory n passing through with the volume transport F_n . The entering wall of the trajectory is coloured green, while the exit wall is coloured red. $T_{i,j,k,n}^{in}$ marks a tracer value at entrance (e.g. temperature or salinity), while $T_{i,j,k,n}^{out}$ marks the tracer value as the trajectory n leaves the grid box (i, j, k) . Grey arrows indicate other trajectories passing through the grid box.

5.1.2 Lagrangian discretisation

In the following section the Eulerian divergence in Equation (5.8) is translated into a Lagrangian view using Lagrangian trajectories and their volume transport. The volume transport (F_n) of a Lagrangian trajectory (n) in TRACMASS is set by the velocity and area of the starting grid box. For example: A trajectory starting at a latitudinal section will have a volume transport accordingly:

$$F_n = v_{i,j,k,t} \Delta x_{i,j} \Delta z_{i,j,k,t} |_{initial}, \quad (5.9)$$

where $v_{i,j,k,t}$ is the velocity at the latitudinal section, $\Delta x_{i,j}$ and $\Delta z_{i,j,k,t}$ are the longitudinal and vertical lengths of the grid box and t is the time-step. The volume transport is thus given in $\text{m}^3 \text{s}^{-1}$. Since the TRACMASS scheme is mass conserving, the trajectory will keep the same volume transport throughout the simulation.

As the trajectory is integrated in time it will pass through several grid boxes. Now, imagine that the trajectory n passes through one grid-box (i, j, k) , with a volume transport F_n , as illustrated in Figure 5.2. The temperature, salinity and density of the trajectory are set by the Eulerian field. These tracers are, however, well mixed in a grid box (stored on T-points on a C-grid as illustrated in Figure 5.1). On the wall, the tracers are averaged between the two nearest grid boxes in TRACMASS. Following the illustration in Figure 5.2, the change in temperature, salinity and density¹ of the trajectory passing through the grid box will be set by:

$$\Delta\Theta_{i,j,k,n} = \Theta_{i,j,k,n}^{out} - \Theta_{i,j,k,n}^{in}, \quad (5.10)$$

$$\Delta S_{i,j,k,n} = S_{i,j,k,n}^{out} - S_{i,j,k,n}^{in}, \quad (5.11)$$

$$\Delta\rho_{i,j,k,n} = \rho_{i,j,k,n}^{out} - \rho_{i,j,k,n}^{in}, \quad (5.12)$$

where $\Theta_{i,j,k,n}^{in}$, $S_{i,j,k,n}^{in}$ and $\rho_{i,j,k,n}^{in}$ are the temperature, salinity and density of the trajectory as it enters the grid box, and $\Theta_{i,j,k,n}^{out}$, $S_{i,j,k,n}^{out}$ and $\rho_{i,j,k,n}^{out}$ are the temperature, salinity and density of the trajectory when it leaves the box. The trajectory's temperature, salinity and density flux through the grid box can thus be written as:

$$H_{i,j,k,n}^{\Theta} = F_n \Delta\Theta_{i,j,k,n}, \quad (5.13)$$

$$H_{i,j,k,n}^S = F_n \Delta S_{i,j,k,n}, \quad (5.14)$$

$$H_{i,j,k,n}^{\rho} = F_n \Delta\rho_{i,j,k,n}, \quad (5.15)$$

where F_n is the volume transport of trajectory n , set at start.

In the same grid box, several more trajectories will pass through, and the total temperature, salinity and density flux in the box can be computed by summing over all trajectories accordingly:

$$H_{i,j,k}^{\Theta} = \sum_n F_n \Delta\Theta_{i,j,k,n}, \quad (5.16)$$

$$H_{i,j,k}^S = \sum_n F_n \Delta S_{i,j,k,n}, \quad (5.17)$$

$$H_{i,j,k}^{\rho} = \sum_n F_n \Delta\rho_{i,j,k,n}. \quad (5.18)$$

Comparing Equations (5.16)-(5.18) with Equation (5.8) reveal that the numerator in Equation (5.8), which describes the tracer flux in and out of a grid box, can be translated to Equations (5.16)-(5.18) for Lagrangian trajectories. Thus, by dividing Equations (5.16)-(5.18) with the volume of the grid box, one will obtain the Lagrangian divergence:

¹In this thesis σ_0 is used.

$$H_{i,j,k}^{\Theta} = \sum_n \frac{F_n \Delta \Theta_{i,j,k,n}}{\Delta x_{i,j} \Delta y_{i,j} \Delta z_{i,j,k,n}}, \quad (5.19)$$

$$H_{i,j,k}^S = \sum_n \frac{F_n \Delta S_{i,j,k,n}}{\Delta x_{i,j} \Delta y_{i,j} \Delta z_{i,j,k,n}}, \quad (5.20)$$

$$H_{i,j,k}^{\rho} = \sum_n \frac{F_n \Delta \rho_{i,j,k,n}}{\Delta x_{i,j} \Delta y_{i,j} \Delta z_{i,j,k,n}}. \quad (5.21)$$

Note that $\Delta z_{i,j,k,n}$, which is the vertical thickness of the grid box, has an index n . This is because the thickness varies in time, and will thus be different for different trajectories that are passing through the grid box. Equations (5.19)-(5.21) describe the Lagrangian divergence of temperature, salinity and density and are directly comparable with the Eulerian divergence (Equation (5.8)).

The Lagrangian divergence can be expressed as a heat, salt and density flux in a latitude-longitude perspective as follows:

$$H_{i,j}^{\Theta} = \frac{\rho_0 c_p}{\Delta x_{i,j} \Delta y_{i,j}} \sum_k \sum_n F_n \Delta \Theta_{i,j,k,n}, \quad (5.22)$$

$$H_{i,j}^S = \frac{1}{1000} \frac{\rho_0}{\Delta x_{i,j} \Delta y_{i,j}} \sum_k \sum_n F_n \Delta S_{i,j,k,n}, \quad (5.23)$$

$$H_{i,j}^{\rho} = \frac{1}{\Delta x_{i,j} \Delta y_{i,j}} \sum_k \sum_n F_n \Delta \rho_{i,j,k,n}, \quad (5.24)$$

where $\rho_0 = 1026 \text{ kg m}^{-3}$ is the density of sea water and $c_p = 3992 \text{ J K}^{-1} \text{ kg}^{-1}$ is the specific heat for water. The Lagrangian divergence of heat, salt and density are now expressed as a heat, salt and buoyancy flux.

6. A summary on the Lagrangian perspective of the ocean circulation

In this chapter follows a summary of the main results presented in this thesis.

6.1 The Lagrangian thermohaline stream function (Paper I and Paper II)

The Conveyor Belt Cell in the Eulerian thermohaline stream function has a warming and a cooling branch. But, where does this cooling and warming mainly take place in the ocean? From an Eulerian perspective it is not straight forward how to connect the stream function with specific geographical regions. However, by tracing specific pathways with Lagrangian trajectories, the main contributing regions can be found.

The northward flowing water in the Atlantic Ocean reflects large parts of the cooling and freshening seen in the stream function (orange contours in Figure 6.1). Similarly, water originating from the Drake Passage, travelling with the ACC and flowing northwards into the Atlantic, Pacific and Indian Oceans mainly contributes to the warming and salinification seen in the thermohaline stream function (blue contours in Figure 6.1).

There is a small discrepancy between the Eulerian and the Lagrangian stream functions. A Lagrangian and Eulerian stream function will never match perfectly due to the different time-averaging in the approaches. In the Eulerian computation, the field is averaged over a selected time period. For the Lagrangian view, on the other hand, the time-scale varies for each trajectory, since each trajectory has a different residence time.

Furthermore, there may be other water masses that contribute to the warming and cooling branches. However, it is clear that those waters play less of a role than the water studied here.

6.2 Cooling and freshening (Paper I)

The northward flowing water in the Atlantic Ocean is mainly cooling in the Gulf Stream, in the northern flank of the Subtropical Gyre and in the North

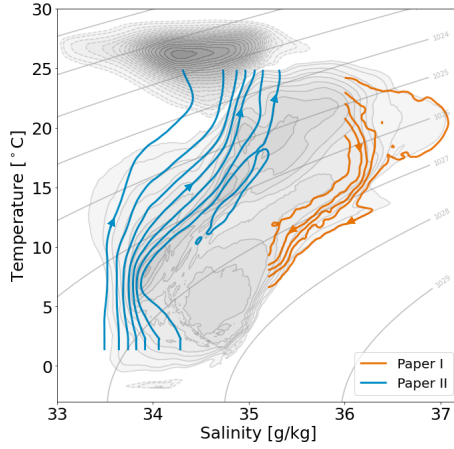


Figure 6.1: The Lagrangian thermohaline stream function for the northward flowing water in the Atlantic Ocean (orange contours) and the northward flowing water in the Southern Ocean (blue contours). The contour interval is 2 Sv, starting from 1 Sv. Grey contours show the Eulerian thermohaline stream function. The contour interval for the Eulerian thermohaline stream function is 2 Sv, where positive contours start from 1 Sv. The figure is adapted from **Paper I** and **Paper II**.

Atlantic Current (Figure 6.2a). Alongside a general cooling, a freshening is seen in the northern flank of the Subtropical Gyre and the North Atlantic Current (Figure 6.2b). Whether this cooling and freshening purely result from air-sea interaction, or a combined effect of air-sea interaction and mixing, is still unclear. However, some ideas are presented in **Paper I**. One representative trajectory indicates a downward spiralling pattern in the Subtropical Gyre, suggesting ocean mixing as one reason for changes in heat and salt at depths. Furthermore, water originating from the northern Atlantic Ocean (e.g. Labrador water) is warming and getting more saline in the same regions as this cooling and freshening is shown, which suggests a mixing between these water masses.

6.3 Warming and salinification (Paper II)

The water from the Drake Passage, that ends as 25°C in the Atlantic, Pacific and Indian Oceans, is warming and salinifying along its path (Figure 6.3). A combination of air-sea interaction, sea-ice-ocean interaction and internal mixing cause this change in heat and salt. In the ACC, the water is cooling in the mixed layer, while below it is warming (Figure 6.3). However, during Austral spring and summer, the mixed layer is thin, while it increases in depth during

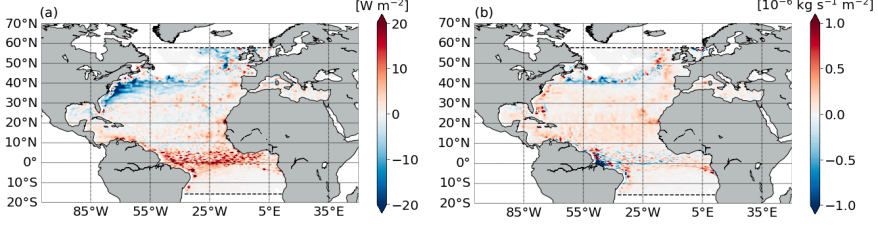


Figure 6.2: (a) The Lagrangian divergence of heat for the northward flowing water in the Atlantic Ocean. (b) The Lagrangian divergence of salt for the same water. The figure is adapted from **Paper I**.

Austral winter and fall. This contributes to a compensation of warming and cooling between seasons, where parcels are warming below the thin mixed layer and cooling in the deeper mixed layer. Similar results are found for salinity, with the additional effect of sea-ice variations and transports.

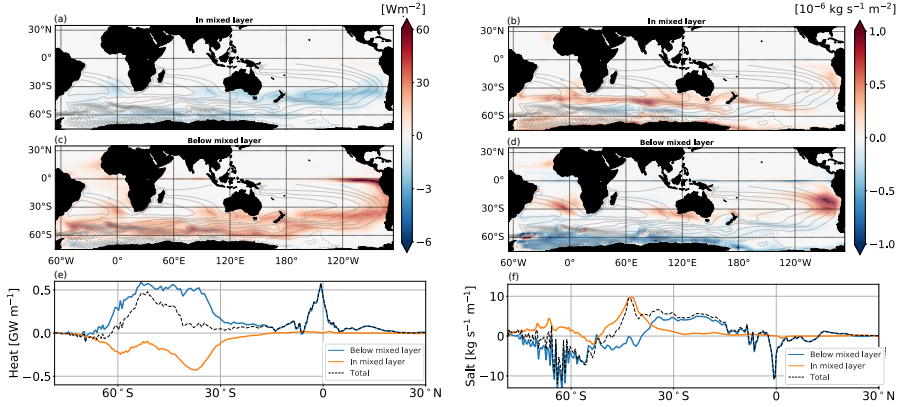


Figure 6.3: (a) The Lagrangian divergence of heat in the momentary mixed layer. The momentary mixed layer depth is the mixed layer for the trajectory at that specific point and time in the simulation. (b) The Lagrangian divergence of salt in the momentary mixed layer. (c) The Lagrangian divergence of heat below the momentary mixed layer. (d) The Lagrangian divergence of salt below the momentary mixed layer. Superimposed on (a)-(d) is the Lagrangian barotropic stream function. (e) The zonally averaged Lagrangian divergence for heat in the mixed layer (blue line) and below mixed layer (orange line). The dashed black line shows the total zonally averaged Lagrangian divergence. (f) Same but for salt. The figure is adapted from **Paper II**.

In the eastern flank of the Southern Hemispheric Subtropical Gyres and along the equator, warming and salinification are mainly found at depth. Thus, this leads to the conclusion that air-sea interaction play less of a role, while internal mixing is the main contributor to changes in these regions.

6.4 The role of the North Atlantic Subtropical Gyre (Paper III)

The North Atlantic Subtropical Gyre (referred to Subtropical Gyre in this section) plays a significant role for the AMOC. 70% of the water that flows northwards as part of the AMOC circulates the Subtropical Gyre up to 14 times before it continues northwards, both denser and deeper compared to when it entered. A mean trajectory, computed from several trajectories that circuit the Subtropical Gyre, reveals that the water in the Subtropical Gyre becomes denser and thus spirals downwards (Figure 6.4). A combination of air-sea interaction and mixing is leading to cooling and freshening, making the water denser for each circuit. These circuits are thus needed for the water to become dense and deep before it continues northwards. These results point to an important role of the Subtropical Gyre to the AMOC, which may be needed to understand to fully predict the state of AMOC in a changing climate.

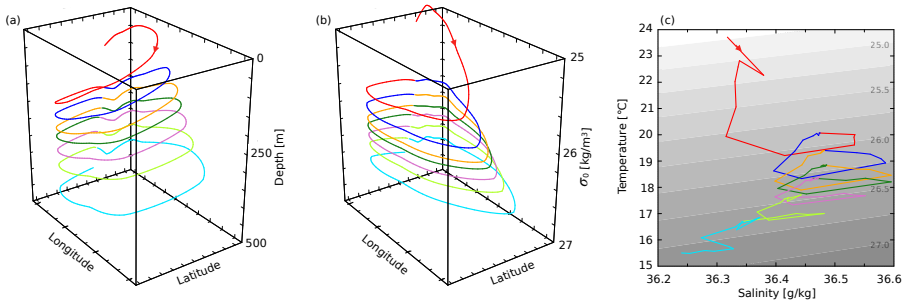


Figure 6.4: A mean trajectory spiralling in the Subtropical Gyre. (a) 3D visualisation of the trajectory with depth. (b) Same as in (a) but with the vertical coordinate density σ_0 . (c) The mean trajectory visualised in temperature-salinity space. Gray shadings show isolines of σ_0 . The figure is adopted from **Paper III**.

6.5 The North Atlantic Ocean circulation (Paper IV)

The circulation in the North Atlantic Ocean are categorised by four different pathways using Lagrangian trajectories, namely: (1) Water originating from the equator that returns to the equator. (2) Water originating from the equator that reaches the subpolar North Atlantic Ocean. (3) Water that originates from the subpolar North Atlantic Ocean, and returns there. (4) Water originating from the subpolar North Atlantic Ocean, that reaches the equator (Figure 6.5). The circulation within the Subtropical Gyre mainly constitutes the northward flowing water in the basin. The North Atlantic Deep Water is spread out in the northern parts of the basin, but as it reaches south of 30°N it is confined

along the deep western boundary current (Figure 6.5a).

The northward flowing water in the basin is freshening and losing heat north of 40°N , while the opposite is true for the water originating from the north (red contours in Figure 6.5). Since this is happening in the same regions, it suggests that there is an exchange of heat and salt between the waters.

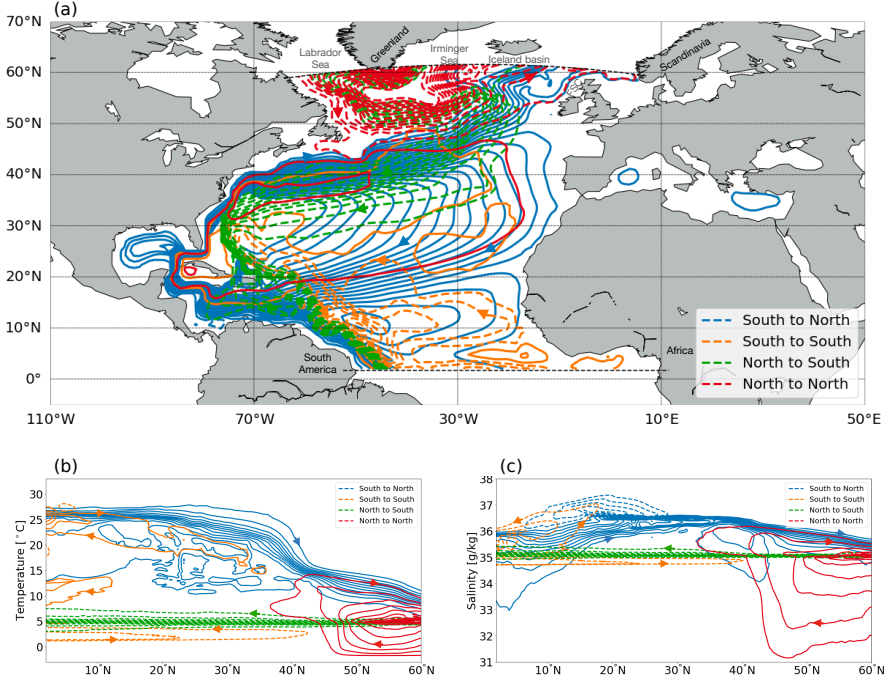


Figure 6.5: (a) The Lagrangian barotropic stream function computed for four different pathways in the North Atlantic Ocean. (b) The Meridional overturning stream function expressed with temperature as coordinate for the four pathways in a. (c) Same as in b but with salinity as coordinate. The contour interval is 2 Sv . Solid contours are clockwise and start at 1 Sv , whereas dashed contours are counter-clockwise and start at -1 Sv . The figure is adapted from **Paper IV**.

7. Final remarks and Outlook

The results in this thesis bring new perspectives to ocean circulation patterns. Figure 7.1 shows a schematic, summarising the pathways that are traced with Lagrangian trajectories. The results provide a detailed picture of regions that are important for heat and salt changes contributing to the changes in density that are driving to the ocean circulation. It is clear that both in the Southern and Northern Hemispheres, the Subtropical Gyres play an important role in transporting water, but also in changing their water mass properties, such as temperature and salinity.

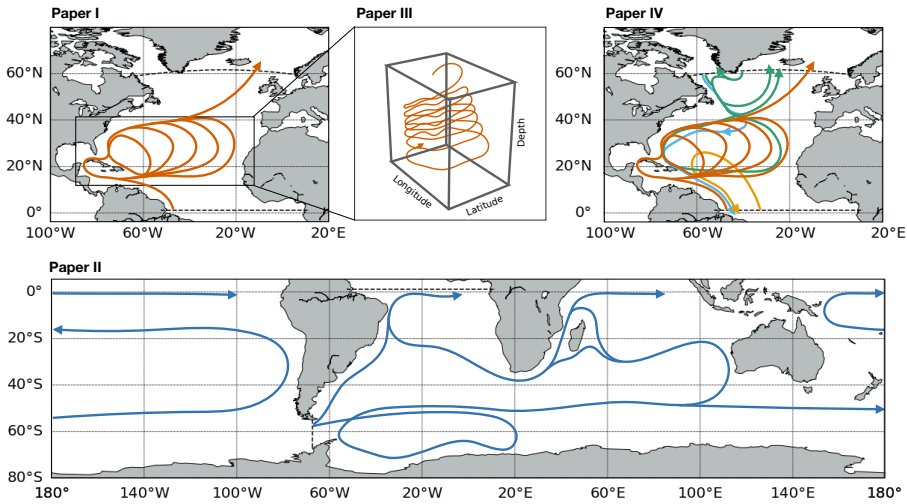


Figure 7.1: A schematic of the ocean circulation pathways that are traced with Lagrangian trajectories. **Paper I:** The northward flowing water of the Atlantic Ocean. **Paper II:** The northward flowing water originating from the Drake Passage, flowing with the ACC ending in the Atlantic, Pacific and Indian Ocean as 25°C. **Paper III:** The spiralling North Atlantic Subtropical Gyre. **Paper IV:** Four pathways in the North Atlantic Ocean.

Below follows a list of possible continuations for the results provided in this thesis:

- **Higher resolution.** The ESMs used in the present thesis, the EC-Earth2.2 and EC-Earth-Veg3.3.1.1, consist of the ocean model NEMO with a horizontal resolution of 1° , 42 or 75 depth levels and monthly means. The resolution implies that the model is non-eddying, which thus puts some constraints on the realism of the simulation. For example, the Gulf Stream is an eddying region, and low resolution models usually have difficulties in both producing the right strength and placement of it. Similarly, there is a large discrepancy among models to generate a reasonable strength of the ACC through the Drake Passage. Therefore, it would be beneficial to repeat the studies performed in this thesis with a higher-resolution model, which is not only eddy-permitting but rather eddy-resolving. However, performing climate run experiments with an ESM is computationally expensive and not always run to equilibrium for large parts of the ocean circulation. There is, on the other hand, an increased use of nesting in ESMs, which means that the model explicitly can resolve eddies in specific regions, for example the Gulf Stream (Matthes *et al.*, 2020).

The study in **Paper III** would benefit from a high-resolution model, to be able to understand how the Subtropical Gyre behave as eddies are resolved. Is there a similar amount of transport still designated to circuit the Subtropical Gyre in a high-resolution model?

We have performed a first analysis on this, with an ocean standalone run using NEMO with a resolution of $1/12^\circ$, 75 depth levels and 5-daily time means. This generated a similar spiral in temperature-salinity space as that shown in **Paper III** (Figure 7.2). From a first glance, an increased horizontal resolution does not affect the resulting spiral tremendously. However, these questions need to be addressed in future studies, preferably with an ESM resolving eddies in the Gulf Stream.

- **The Lagrangian divergence.** As described in Chapter 5 and specifically Equation (5.4), the Lagrangian divergence is approximately in balance with the surface fluxes, lateral mixing and vertical mixing. These types of fluxes are all output variables that can be saved in an ESM, usually referred to as tendencies or budget terms of heat and salt. Including these fields in the Lagrangian trajectory code TRACMASS can potentially provide the possibility to trace water and simultaneously study the processes that cause changes in heat and salt. Implementing this type of tracing would open up the feasibility to in detail study processes of water mass transformation globally and regionally.

The studies performed in this thesis would benefit from this type of implementation in TRACMASS. It would then be possible to distinguish regions in the ocean that are more or less important for specific processes causing the water mass transformation, and explicitly understanding where mixing below the mixed layer plays an important role.

- **Future climates.** The Subtropical Gyre plays a crucial role in recirculating and densifying the water flowing northwards as part of the

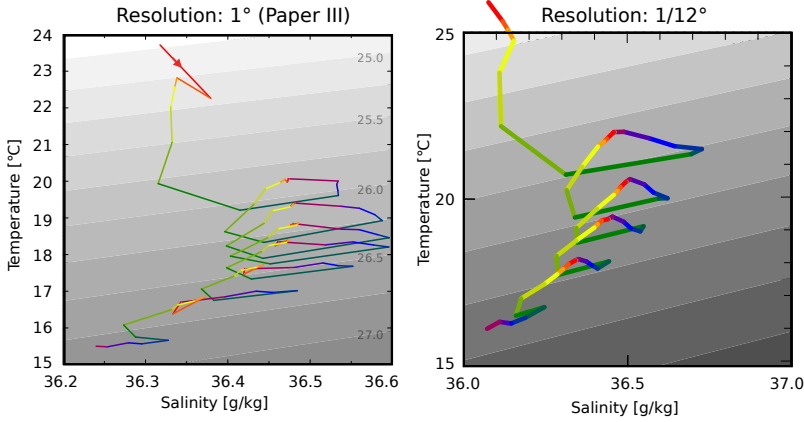


Figure 7.2: (a) The mean trajectory of the Subtropical Gyre that were presented in **Paper III** where data from the ESM EC-Earth-Veg3.3.1.1 were used with a resolution of 1° for the ocean. Figure adopted from **Paper III**. (b) The same mean trajectory, but computed for an ocean standalone simulation using NEMO with a resolution of $1/12^\circ$. Note that the temperature and salinity axes span different values.

AMOC (**Paper III**). As climate is changing with the increase of anthropogenic greenhouse gases, the circulation, temperature and salinity distribution in the Subtropical Gyre is expected to change (Bindoff *et al.*, 2019). What implications this would have on the downward spiralling Subtropical Gyre and the related changes in temperature and salinity are unclear. One can, however, expect that climate-related changes will have an impact on the system. Therefore, performing a similar analysis as that undertaken in **Paper III** for future scenarios would be interesting.

- **The role of ocean gyres.** What role do other ocean gyres play for the ocean circulation? There are several gyres that are not included in the pathways of this thesis. It is clear from our results, that the North Atlantic Subtropical Gyre consists of water moving northwards as the upper branch of AMOC, while most other waters of the Atlantic Ocean do not circulate the gyre. Similarly, other ocean gyres may transport specific water masses. The water followed in the Southern Hemisphere does not circulate in the Subtropical Gyres, but rather moves directly northwards. Lagrangian trajectories could be used to trace water masses that are circulating the ocean gyres, and potentially provide a new insight to the gyre circulation.
- **The thermohaline stream function.** As seen in Figure 6.1, some parts of the thermohaline stream function are not covered within the studies performed in **Paper I** and **Paper II**. Tracing the rest of the thermohaline circulation should probably be divided into different studies, since

the circulation consist of different water masses and probably covers different geographical regions. The Tropical Cell is suggested to result from the circulation in the Pacific warm pool (Döös *et al.*, 2012), thus Lagrangian trajectories simulated through the Tropical Pacific Ocean may bring clarity into this circulation pattern.

Further, closing the Conveyor Belt Cell at cold temperatures would be beneficial to understand where the rest of the cooling and freshening takes place. This could also bring clarity in how the warming and cooling branch of the Conveyor Belt Cell are connected with each other. Finally, it would provide an understanding to how deep water appears in the thermohaline stream function.

Finally, water in the ACC is changing its temperature and salinity as it travels around Antarctica, resulting in a thermohaline circulation in the stream function. A water parcel can further circuit the ACC one or several times, similar to the Subtropical Gyre circulation. This could potentially lead to different thermohaline properties depending on the amount of circuits performed. Thus, another way of understanding the circulation in the ACC and its appurtenant temperature and salinity changes are by tracing parcels that perform a different number of circuits.

References

- ALDAMA CAMPINO, A. (2019). *Atmospheric and oceanic circulation from a thermodynamic perspective*. Ph.D. thesis, Department of Meteorology, Stockholm University. 24
- ALDAMA CAMPINO, A., FRANSNER, F., ÖDALEN, M., GROESKAMP, S., YOOL, A., DÖÖS, K. & NYCANDER, J. (2020). Meridional ocean carbon transport. *Global Biogeochemical Cycles*, **34**, e2019GB006336. 24
- BINDOFF, N.L., CHEUNG, W.W., KAIRO, J.G., ARISTEGUI, J., GUINDER, V.A., HALLBERG, R., HILMI, N.J.M., JIAO, N., KARIM, M.S., LEVIN, L. *et al.* (2019). Changing Ocean Marine Ecosystems, and Dependent Communities. In: IPCC Special Report on the Ocean and Cryosphere in a Changing Climate.[H.-O. Pörtner, D.C. Roberts, V. Masson-Delmotte, P. Zhai, M. Tignor, E. Poloczanska, K. Mintenbeck, A. Alegría, M. Nicolai, A. Okem, J. Petzold, B. Rama, N.M. Weyer]. *IPCC*, 477–587. 13, 18, 41
- BLANKE, B. & RAYNAUD, S. (1997). Kinematics of the pacific equatorial undercurrent: An eulerian and lagrangian approach from gcm results. *Journal of Physical Oceanography*, **27**, 1038–1053. 21
- BLANKE, B., ARHAN, M., MADEC, G. & ROCHE, S. (1999). Warm water paths in the equatorial atlantic as diagnosed with a general circulation model. *Journal of Physical Oceanography*, **29**, 2753–2768. 24
- BRUNET, G., SHAPIRO, M., HOSKINS, B., MONCRIEFF, M., DOLE, R., KILADIS, G.N., KIRTMAN, B., LORENC, A., MILLS, B., MORSS, R. *et al.* (2010). Collaboration of the weather and climate communities to advance subseasonal-to-seasonal prediction. *Bulletin of the American Meteorological Society*, **91**, 1397–1406. 20
- BRYAN, K. (1969). Climate and the ocean circulation: Iii. the ocean model. *Monthly Weather Review*, **97**, 806–827. 13
- BUCKLEY, M.W. & MARSHALL, J. (2016). Observations, inferences, and mechanisms of the atlantic meridional overturning circulation: A review. *Reviews of Geophysics*, **54**, 5–63. 23
- CAESAR, L., MCCARTHY, G., THORNALLEY, D., CAHILL, N. & RAHMSTORF, S. (2021). Current Atlantic meridional overturning circulation weakest in last millennium. *Nature Geoscience*, 1–3. 18
- CHEN, ROJAS, SAMSET, COBB, NIANG, D., EDWARDS, EMORI, FARIA, HAWKINS, HOPE, HUYBRECHTS, MEINSHAUSEN, MUSTAF, PLATTNER & TRÉGUIER (2021). Framing, context, and methods. In: Climate Change 2021: The Physical Science Basis. Contribution of Working Group I to the Sixth Assessment Report of the Intergovernmental Panel on Climate Change.[Masson-Delmotte V. P. Zhai A. Pirani S.L. Connors C. Péan S. Berger N. Caud Y. Chen L. Goldfarb M.I. Gomis M. Huang K. Leitzell E. Lonnoy J.B.R. Matthews T.K. Maycock T. Waterfield O. Yelekçi R. Yu and B. Zhou (eds.)]. *IPCC*. 19
- CUNNINGHAM, S.A., KANZOW, T., RAYNER, D., BARINGER, M.O., JOHNS, W.E., MAROTZKE, J., LONGWORTH, H.R., GRANT, E.M., HIRSCHI, J.J.M., BEAL, L.M. *et al.* (2007). Temporal variability of the atlantic meridional overturning circulation at 26.5 n. *science*, **317**, 935–938. 13
- DE VRIES, P. & DÖÖS, K. (2001). Calculating lagrangian trajectories using time-dependent velocity fields. *Journal of Atmospheric and Oceanic Technology*, **18**, 1092–1101. 21
- DÖÖS, K. (1995). Inter-ocean exchange of water masses. *Journal of Geophysical Research: Oceans*, **100**, 13499–13514. 21

- DÖÖS, K. & WEBB, D.J. (1994). The deacon cell and the other meridional cells of the southern ocean. *Journal of Physical Oceanography*, **24**, 429–442. 23, 24
- DÖÖS, K., NYCANDER, J. & COWARD, A.C. (2008). Lagrangian decomposition of the deacon cell. *Journal of Geophysical Research: Oceans*, **113**. 24
- DÖÖS, K., NILSSON, J., NYCANDER, J., BRODEAU, L. & BALLAROTTA, M. (2012). The world ocean thermohaline circulation. *Journal of Physical Oceanography*, **42**, 1445–1460. 24, 42
- DÖÖS, K., JÖNSSON, B. & KJELLSSON, J. (2017a). Evaluation of oceanic and atmospheric trajectory schemes in the tracmass trajectory model v6. 0. *Geoscientific Model Development*, **10**, 1733–1749. 21, 25
- DÖÖS, K., KJELLSSON, J., ZIKA, J., LALIBERTÉ, F., BRODEAU, L. & CAMPINO, A.A. (2017b). The coupled ocean–atmosphere hydrothermohaline circulation. *Journal of Climate*, **30**, 631–647. 24
- DÖSCHER, R., ACOSTA, M., ALESSANDRI, A., ANTHONI, P., ARNETH, A., ARSOUZE, T., BERGMANN, T., BERNADELLO, R., BOUSETTA, S., CARON, L.P. *et al.* (2021). The ec-earth3 earth system model for the climate model intercomparison project 6. *Geoscientific Model Development Discussions*, 1–90. 20
- DRIJFHOUT, S., DE VRIES, P., DÖÖS, K. & COWARD, A. (2003). Impact of eddy-induced transport on the lagrangian structure of the upper branch of the thermohaline circulation. *Journal of Physical Oceanography*, **33**, 2141–2155. 24
- DÖÖS, K., LUNDBERG, P. & CAMPINO, A.A. (2021). *Basic Numerical Methods in Meteorology and Oceanography*. in press, Stockholm University Press. 27
- EKMAN, V.W. (1905). On the influence of the earth's rotation on ocean-currents. *Ark. Math. Aston. Fys.*, **2**, 1–53. 16
- FEDAK, M. (2004). Marine animals as platforms for oceanographic sampling: a "win/win" situation for biology and operational oceanography. *Mem. Natl Inst. Polar Res.*, **58**, 133–147. 13, 19
- FRIOCOURT, Y., DRIJFHOUT, S., BLANKE, B. & SPEICH, S. (2005). Water mass export from Drake Passage to the Atlantic, Indian, and Pacific oceans: a Lagrangian model analysis. *Journal of physical oceanography*, **35**, 1206–1222. 24
- GROESKAMP, S., ZIKA, J.D., MCDUGALL, T.J., SLOYAN, B.M. & LALIBERTÉ, F. (2014). The representation of ocean circulation and variability in thermodynamic coordinates. *Journal of Physical Oceanography*, **44**, 1735–1750. 24
- HAARSMA, R.J., ROBERTS, M.J., VIDALE, P.L., SENIOR, C.A., BELLUCCI, A., BAO, Q., CHANG, P., CORTI, S., FÜCKAR, N.S., GUEMAS, V. *et al.* (2016). High resolution model intercomparison project (highresmip v1. 0) for cmip6. *Geoscientific Model Development*, **9**, 4185–4208. 19
- HIERONYMUS, M., NILSSON, J. & NYCANDER, J. (2014). Water mass transformation in salinity–temperature space. *Journal of Physical Oceanography*, **44**, 2547–2568. 24
- LOZIER, M.S. (2012). Overturning in the North Atlantic. *Annual review of marine science*, **4**, 291–315. 18
- MANABE, S. (1969a). Climate and the ocean circulation: I. the atmospheric circulation and the hydrology of the earth's surface. *Monthly Weather Review*, **97**, 739–774. 13
- MANABE, S. (1969b). Climate and the ocean circulation: II. the atmospheric circulation and the effect of heat transfer by ocean currents. *Monthly Weather Review*, **97**, 775–805. 13
- MATTHES, K., BIASTOCH, A., WAHL, S., HARLASS, J., MARTIN, T., BRÜCHER, T., DREWS, A., EHLERT, D., GETZLAFF, K., KRÜGER, F. *et al.* (2020). The flexible ocean and climate infrastructure version 1 (focli): mean state and variability. *Geoscientific Model Development*, **13**, 2533–2568. 40
- MUNK, W.H. (1950). On the wind-driven ocean circulation. *Journal of Atmospheric Sciences*, **7**, 80–93. 17
- NYCANDER, J., NILSSON, J., DÖÖS, K. & BROSTRÖM, G. (2007). Thermodynamic analysis of ocean circulation. *Journal of physical oceanography*, **37**, 2038–2052. 24
- RAHMSTORF, S. (2003). Thermohaline circulation: The current climate. *Nature*, **421**, 699–699. 17

- RAHMSTORF, S., BOX, J.E., FEULNER, G., MANN, M.E., ROBINSON, A., RUTHERFORD, S. & SCHAFFERNICHT, E.J. (2015). Exceptional twentieth-century slowdown in Atlantic ocean overturning circulation. *Nature climate change*, **5**, 475–480. 18
- RICHARDSON, P.L. (2008). On the history of meridional overturning circulation schematic diagrams. *Progress in Oceanography*, **76**, 466–486. 15
- SANDSTRÖM, J.W. (1908). Dynamische versuche mit meerwasser. *Annal. Hydrogr. Marit. Meteorol.*, **36**, 6–23. 17
- STOMMEL, H. (1948). The westward intensification of wind-driven ocean currents. *Eos, Transactions American Geophysical Union*, **29**, 202–206. 17
- SVERDRUP, H.U. (1947). Wind-driven currents in a baroclinic ocean; with application to the equatorial currents of the eastern pacific. *Proceedings of the National Academy of Sciences of the United States of America*, **33**, 318. 17
- SVERDRUP, K.A., DUXBURY, A.C. & DUXBURY, A. (2005). *An introduction to the world's oceans*. McGraw-Hill Higher Education. 13
- THOMAS, M.D., TRÉGUIER, A.M., BLANKE, B., DESHAYES, J. & VOLDOIRE, A. (2015). A lagrangian method to isolate the impacts of mixed layer subduction on the meridional overturning circulation in a numerical model. *Journal of Climate*, **28**, 7503–7517. 24
- TRACMASS (2021). Tracmass. <http://www.tracmass.org>. 21
- VALLIS, G.K. (2017). *Atmospheric and oceanic fluid dynamics*. Cambridge University Press. 16, 18, 23
- VAN SEBILLE, E., GRIFFIES, S.M., ABERNATHEY, R., ADAMS, T.P., BERLOFF, P., BIASTOCH, A., BLANKE, B., CHASSIGNET, E.P., CHENG, Y., COTTER, C.J. *et al.* (2018). Lagrangian ocean analysis: Fundamentals and practices. *Ocean Modelling*, **121**, 49–75. 13
- WEIJER, W., CHENG, W., GARUBA, O.A., HU, A. & NADIGA, B. (2020). CMIP6 models predict significant 21st century decline of the Atlantic meridional overturning circulation. *Geophysical Research Letters*, **47**, e2019GL086075. 18
- ZIKA, J.D., ENGLAND, M.H. & SLP, W.P. (2012). The ocean circulation in thermohaline coordinates. *Journal of Physical Oceanography*, **42**, 708–724. 24

Acknowledgements

This has been an amazing journey (it is impossible to understand that its actually about to end), and it would not have been possible without the support and help from many. This acknowledgement is not enough to thank you all for what you have done for me, but I will give it a try.

My supervisor, **Kristofer Döös**, there are not words enough that can express my gratitude to you. I am extremely thankful that I got the possibility to do this PhD with you as my supervisor. Thank you for believing in me and supporting me. You have taught me a lot during these years. However, I do think I have taught you some things as well. For me, you have been the best supervisor I could ever wished for.

My other supervisor, **Jonas Nycander**. Thank you for all the interesting discussions and all the inspiration you have given me. I have learned a lot from you!

Aitor Aldama Campino, I am not sure I will be able to express my gratitude to you. I am so glad that I got finish this PhD with you still around at MISU. We have gone through many years together, always supporting each other in all kind of situations. Thank you for all our discussions and a special thank you for always remembering everything I do not manage to remember. Never forget how great you are! I hope you will cope with all my questions in the future as well.

Another special thank you to my dearest colleague, **Dipanjan Dey**. You have been a true inspiration for me. I am so impressed by everything you do. I wish you all the best in your future!

Ezra Eisbrenner, it has been a pleasure getting to know you. I wished we would have had more time at MISU together. Thank you for all the support you have given me! I wish you all the best with your PhD.

The biggest thank you to the Ocean group at MISU. First of all, I am extremely happy that I got to share my time at MISU with this amazing group of people. All oceanographers at MISU, you are the best! My fellow PhDs, **Gaspard Geoffroy**, **Jonathan Wiskandt** and **Aunraj Kondentharayil Soman** thank you for all the inspiration and joy you have given me. I wish you all the best in the future, you rock! **Johan Nilsson**, **Inga Kozalska** and **Léon Chafik** I am very thankful for all of you, especially your openness and kindness in sharing your experiences. Thank you! Do not forget to keep up the ocean meetings now!

Karolina Siegel, I would not have kept my sanity without some of our long discussions about life. Thank you!

Sonja Murto, never stop believing in yourself. You are such an incredible

person, I have never met anyone who cares so much about everyone around. Thank you for all our long discussions about life.

To all my fellow **PhDs at MISU**, thank you all for being such an amazing group of people. I am forever thankful that I got the possibility to meet and get inspired by all of you. I wish you all the best in the future.

Anna Lewinschal, thank you for all the support you have given me! Especially while I learned to run a climate model. I would not have done it without you! I look forward to the day you teach me how to knit.

Ingrid Eronn, I am so grateful for our working-out sessions! I hope we will be able to continue with this at some point.

A special thank you to you, **Frida Bender**. I am not sure you have understood what an inspiring person you are, in so many ways.

Susanne Ericson, thank you for always answering all my questions with a big smile.

To my committee members at MISU, **Susanne Benze**, **Abdel Hannachi** and **Bodil Karlsson**. Thank you for supporting me and helping me move forward in my studies.

I have changed office several times during my time at MISU, and have had the pleasure to share office with many incredible persons. Thank you all for all our times! A special thank you to **Lina Broman**, unfortunately we did not get to share the office for too long, but I have had so many great moments with you, sharing experiences and supporting each other. I wish you all the best in life!

Further, I would like to thank **everyone at MISU**, both existing colleagues and long gone. MISU would not have been the same without you. Many of you I had already as a Bachelor student; thank you for inspiring me to continue with science! I hope you will continue to inspire many more scientists out there. I am forever grateful that I got to spend all these years with all of you.

Peter Lundberg, thank you for always taking your time to help me and support me, especially with writing.

Sjoerd Groeskamp and **Trevor J. McDougall**, I want to add a special thanks to you two, my first two co-authors outside of MISU. You have been a big inspiration, and I am truly happy I got the possibility to work with such amazing people like you two. Thank you for everything! I look forward to continue our collaboration, and I hope we will be able to do it in person at some point!

A big thank you to **Joakim Kjellsson**, for all the support during these years, teaching me git, TRACMASS and so much more.

Sara Broomé and **Malin Ödalen**, I do not have words enough to express how much you mean to me. I am so thankful that I got the luxury of meeting you two. Wherever we are in the world, I know we will be true friends for life. You both have been the best support I could ever have wished for during this journey. I look forward to all our future adventures together!

Eva Nygrén, you are an amazing, inspiring, fun person and I have learned so much from you, especially in handling motherhood. Continue to be you,

forever.

There is one person out there, who put me here already as a teenager. **Janne**, without your endless engagement in my studies I would never have reached this far. There are no words enough to explain how much you did for me. You made me love maths and physics. Thank you!

To my beloved friends, **Melanie, Marcus, Staven, Emelie, Isabelle and Christian**. Thank you for always being there, believing in me, supporting me and just being the best friends one could wish for! **Melanie**, thank you for always caring, listening and just being there. You are such a wonderful friend!

Malva, Therese, Josefine and Amanda, I can not imagine that I would ever have reached this far without you. Thank you for all our fun times, for always being there and for being who you are. You are amazing friends.

Finally, nothing in this world would be possible without my lovely family. My mum **Eva** and dad **Anders**, you are the best parents. You have inspired me to become who I am today and I am forever grateful. Dad, by always being there and putting life in perspective; have I ever heard you complain about anything? You always put me first and supports me in ways no one else can. Mum, the best grandma in the world, there are no words to express how much you mean to me. My grandma **Inga**, thank you for always being part of my life and always believing in me. You are wonderful! My sister **Hanna**, my biggest inspiration in life. I wished everyone would get the luxury of having a big sister like you. You are always inspiring me into doing my best and to believe in myself. Thank you for everything!

My love **Stefan**, you play such a big role in all of this. All those moments I have felt completely lost, you are always there, making me laugh in the way no one else can. I would never have managed this without your encouragement and love. You are amazing and I look forward to all our adventures together in the future. *I love you!*

Isabella and Alexandra, the best kids in the whole wide world. In times when everything feels overwhelming, you put perspective on what is important in life. Thank you for being you, continue to be like this forever. Never stop believing in yourself. You are the best!